Biochemical and Biophysical Research Communications 427 (2012) 478–484

Contents lists available at SciVerse ScienceDirect

Biochemical and Biophysical Research Communications

journal homepage: www.elsevier.com/locate/ybbrc

Cholesterol-enriched microdomains regulate pseudopod extension in the MSP-based cytoskeleton of amoeboid sperm

Juan J. Fraire-Zamora *, Tung Tran, Richard A. Cardullo *

Department of Biology, University of California, Riverside, CA 92521, United States

ARTICLE INFO

Article history:
Received 11 September 2012
Available online 18 September 2012

Keywords:
Cell motility
Cytoskeleton
Membrane microdomains
Cholesterol
Major sperm protein

ABSTRACT

In the amoeboid spermatozoa from *Caenorhabditis elegans*, motility acquisition is preceded by substantial rearrangement of the plasma membrane. The current genetic model posits a multicomponent complex of membrane and cytoplasmic proteins responsible for pseudopod extension. This model can be translated into a physiological context through the involvement of cholesterol-enriched signaling platforms. We show that discrete cholesterol-enriched microdomains are present in *C. elegans* spermatids. These microdomains redistributed towards the cell body upon pseudopod extension resulting in a phospholipid-enriched pseudopod. Cholesterol saturation in the spermatids prevented pseudopod extension and motility acquisition, whereas cholesterol depletion increased the rate of *in vitro* pseudopod extension. This work suggests that plasma membrane cholesterol plays an important role in regulating the membrane dynamics that precede pseudopod extension and motility acquisition.

1. Introduction

Biological membranes are complex cellular structures responsible for maintaining homeostasis. In particular, the plasma membrane regulates the interactions of a cell to its substrate and adjacent cells. This regulation ultimately depends on both membrane structure and dynamics which can affect the quality, duration, and strength of signaling cascades during cytoskeletal modulation, cell adhesion and motility [1,2].

Spermatozoa from the nematode *Caenorhabditis elegans* are highly motile amoeboid cells that must first undergo a series of substantial membrane rearrangements before motility can be achieved [3,4]. During this physiological process, a spherical sessile spermatid must extend transient membrane protrusions (“spikes”) that can thicken and fuse to coalesce into a pseudopod [5]. Upon pseudopod extension, membrane flow ceases in the cell body, the nematode-specific membranous organelles (MOs) fuse to the cell body plasma membrane, and pseudopodial membrane flow is initiated from the tip to the base rendering a highly fluid and dynamic cell surface [3]. This flow, coupled to dynamic cytoskeleton assembly and disassembly, results in the maintenance of motility in nematode sperm [6,7]. Interestingly, the cytoskeleton of amoeboid spermatozoa does not contain actin or associated motor proteins seen in typical motile eukaryotic cells, instead, amoeboid sperm motility is powered exclusively by the major sperm protein (MSP)-based cytoskeleton rendering this cell type as a simple model system to study the processes of cytoskeletal modulation, cell adhesion and motility compared to the analogous actin-based cytoskeleton [6].

Genetic screens in *C. elegans* have identified proteins responsible for the block/trigger of pseudopod extension. The SPErmatogenesis-defective group of proteins (also known as the SPE-8 group) functions as a multicomponent complex that promotes the interaction of membrane (SPE-12, SPE-19 and SPE-29) and cytoplasmic (SPE-6, SPE-8 and SPE-27) signaling proteins in a common pathway during pseudopod extension [8–13]. Another group of SPE proteins (the SPE-9 group: SPE-9, SPE-38 and TRP-3/SPE-41) rearrange their localization during the spermatid-to-spermatozoa transition [14–17]. Altogether, these events result in a dynamic exchange of diffusible material within the plasma membrane necessary for motility acquisition and fertilization [18]. By integrating both the physiological and genetic evidence for pseudopod extension in nematode sperm, we recently proposed a model that considers the involvement of cholesterol-enriched membrane microdomains as platforms responsible for regulating the spatial and temporal signals during spermatid activation and pseudopod extension [19].

Cholesterol is an important component of the plasma membrane and its structural characteristics enable it to modulate membrane organization and permeability [20]. It has been shown that cholesterol depletion can induce the inhibition of motility in human neutrophils [21], T-cells [22] and breast cancer-derived cells [23] as well as the initiation of a transmembrane signal that results in capacitation of mammalian spermatozoa [24]. In *C. elegans*,

* Corresponding authors. Fax: +1 (951) 827 4286.
E-mail addresses: jfrai001@ucr.edu (J.J. Fraire-Zamora), cardullo@ucr.edu (R.A. Cardullo).

0006-291X/$ - see front matter © 2012 Elsevier Inc. All rights reserved.
http://dx.doi.org/10.1016/j.bbrc.2012.09.071

exogenous cholesterol is required for reproduction and survival since this nematode is unable to synthesize sterols *de novo* [25]. Furthermore, the distribution of sterols in *C. elegans* is not uniform and only a subset of cells, including sperm and oocytes, accumulate cholesterol [26,27]. In the present work, we investigate the localization of cholesterol in *C. elegans* sperm and the effects of cholesterol saturation and depletion on *in vitro* pseudopod extension. Our results suggest that cholesterol plays an important role in regulating the membrane dynamics that precede pseudopod extension and motility acquisition in *C. elegans* amoeboid sperm.

2. Materials and methods

2.1. Genetic strains, worm synchronization and large-scale sperm isolation

C. elegans strain CB1489: *him-8* (e1489) IV was used since *him-8* males produce ~40% male progeny compared to ~0.1% males produced by wild type [28] and their sperm are cytologically indistinguishable from wild-type sperm [29]. Worms were maintained at 20 °C on NGM plates seeded with *Escherichia coli* OP50 as described [30]. Culture synchronization, male separation and large-scale sperm isolation were performed as previously described [31] with some modifications (for a detailed description see Supplementary materials and methods).

2.2. Small-scale sperm isolation method and fluorescent staining

Synchronized young adult males were used to obtain spermatids by cutting the posterior end of worms (for a detailed description see Supplementary materials and methods). Spermatids were fixed and stained with filipin for cholesterol localization or stained with 7-nitrobenz-2-oxa-1,3-diazol-4-yl (NBD) cholesterol or phosphatidylcholine (for details see Supplementary materials and methods). Cells were observed using a fluorescence microscope and images were captured using a Dage-MTI CDC 100 camera mounted onto the microscope and processed using the software Scion Image v. 1.62 from NIH.

2.3. Live cell microscopy

To achieve high magnification video-enhanced contrast (VEC) microscopy and to facilitate *in vitro* activation assays in an inverted microscope, a coverslip perfusion chamber was prepared (see Supplementary materials and methods). For counting purposes, sperm cells were observed using a Nikon Labophot phase contrast microscope with a 40× objective. Images were captured using a Dage-MTI CDC 100 camera and software mentioned above. For live cell imaging purposes, sperm cells were observed using a Zeiss Axiovert 10 microscope equipped with DIC optics and a 100× oil immersion objective (1.3 NA). Images were captured using a Hamamatsu C8484-05G digital CCD camera mounted onto the microscope and analyzed using the software SimplePCI v. 6.1 from Compix Inc., Imaging Systems.

2.4. Statistical analysis

Details on the method used to avoid pseudoreplication in sperm cell counting can be found in the Supplementary materials and methods. Curves from pseudopod extension kinetics were fit by SigmaPlot (Jandel Scientific) using a 4-parameter Hill equation to calculate the half-time of pseudopod extension. Treatments were compared to its corresponding control for each *in vitro* activator using the Student's *t*-test.

3. Results

3.1. Cholesterol-enriched microdomains are present in C. elegans spermatids

To search for cholesterol-enriched microdomains in the spermatids of *C. elegans*, we stained fixed cells using the fluorescent antibiotic filipin that tightly binds to cholesterol in biological membranes. Unactivated spermatids incubated in MSM (to prevent pseudopod extension) displayed discrete regions where filipin is localized, suggesting the presence of cholesterol-enriched membrane microdomains (Fig. 1A, i). Treatment of spermatids (previous to fixation) with the known cholesterol acceptor 2-OH-propyl-β-cyclodextrin (2-OH-CD) depleted these discrete regions in spermatids (Fig. 1A, ii). Due to their hydrophobic nature, insolubility in detergents and light buoyancy, the presence of cholesterol-enriched membrane microdomains in cells can be biochemically accounted for by the isolation of detergent-resistant membrane (DRM) fractions [32]. Thus, we isolated DRMs to corroborate the presence of membrane microdomains in *C. elegans* spermatids. Spermatids isolated in MSM were subjected to detergent extraction and separated using a continuous multi-layer step gradient (see Supplementary materials and methods). Light-buoyant DRMs were observed in the fractions corresponding to 20%, 15% and 10% of the gradient. These DRMs contained at least three bands that migrated at ~40, 30 and 16 kDa, respectively (see Supplementary Fig. SF1). Treatment of spermatids with 2-OH-CD (previous to DRMs isolation) depleted these bands from the light-buoyant fraction. As an indirect way to account for the effect of cholesterol depletion on spermatids, cells were subjected to subcellular fractionation by means of differential centrifugation (see Supplementary materials and methods). Two subcellular fractions can be separated using this method [33], the putative membrane fraction (P100) that consists of plasma membrane and membrane bound vesicles and the putative cytosolic fraction (S100) that contains abundant amounts of the cytoskeletal major sperm protein. Since cholesterol depletion promotes a reorganization of the plasma membrane, we expected to observe a change in the protein pattern or band intensity of treated spermatids. Indeed, when comparing the P100 fraction from cholesterol-depleted and untreated spermatids, we observed a decrease in band intensities of spermatids treated with 2-OH-CD as compared to control spermatids (see Supplementary Fig. SF2). In particular, the intensity of two bands that were also present in the DRM's (~40 and 30 KDa) was greatly reduced upon cholesterol depletion. Altogether, these results indicate the presence of cholesterol-enriched membrane microdomains in the spermatids of *C. elegans* and that cholesterol depletion promotes rearrangement of proteins present in the plasma membrane.

3.2. Cholesterol redistributes during pseudopod extension and controls spermatid activation

To gain insight on the fate of cholesterol during pseudopod extension we followed its dynamics by loading spermatids with the fluorescently labeled cholesterol analog NBD-cholesterol that localized to discrete regions of the spermatid (see Fig. 1B, i and ii, arrowheads). Pseudopod extension was induced in NBD-cholesterol loaded cells using the known *in vitro* activator Pronase. NBD-cholesterol redistributed uniformly to the cell body of the spermatid leaving a cholesterol-free pseudopod (see Fig. 1B, iv and v, arrows). In contrast, spermatids labeled with NBD-phosphatidylcholine (NBD-PC), showed a uniform labeling that included the pseudopod upon spermatid activation (Fig. 1B, iii and vi, arrows). This result suggests that cholesterol-enriched microdomains are present in spermatids prior to activation and that upon pseudopod extension

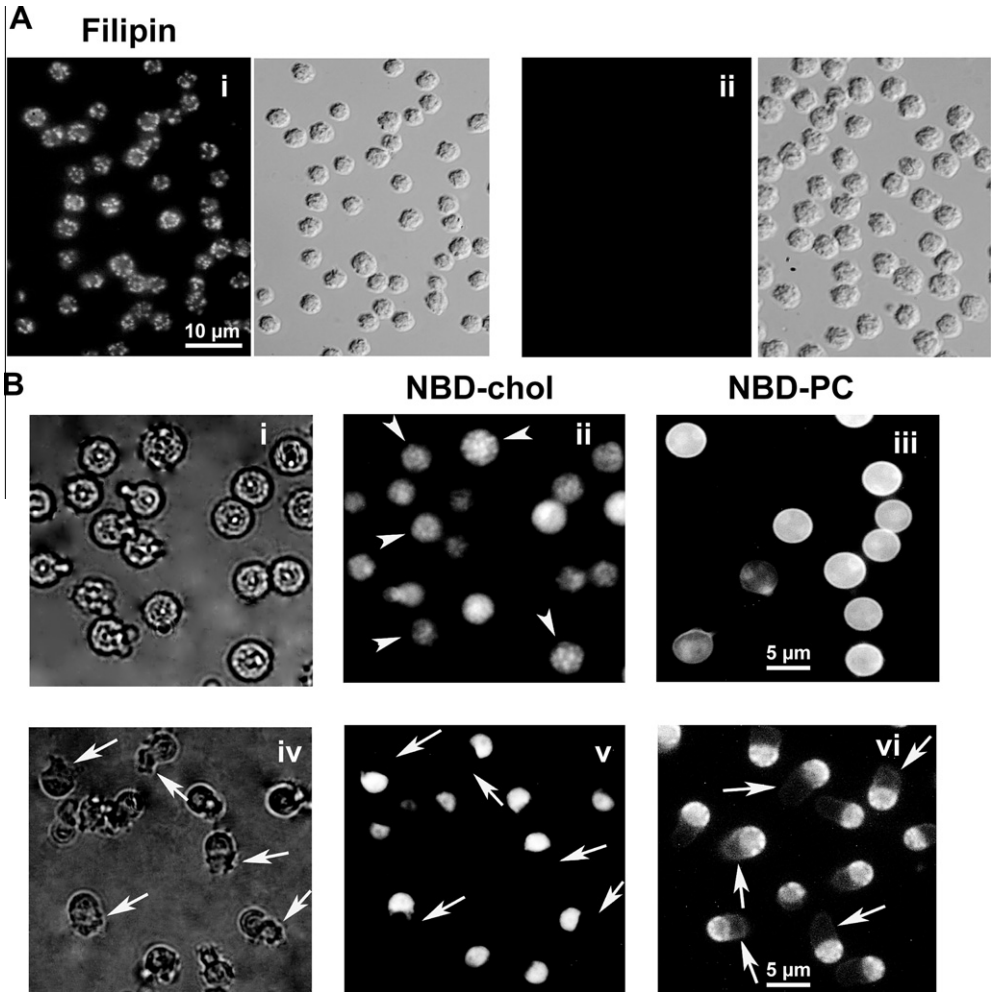

Fig. 1. Cholesterol localization and redistribution during pseudopod extension in *C. elegans* spermatids. A. Cholesterol localization in fixed spermatids. (i) Filipin staining showed discrete punctae of cholesterol-enriched regions on untreated spermatids while treatment with 2-OH-CD (ii) depleted these regions. B. Cholesterol redistribution in live spermatids labeled with NBD fluorescent dyes. (i and ii) Spermatids were labeled with NBD-cholesterol showing accumulation on discrete regions (arrowheads). (iv and v) These discrete punctae redistributed towards the cell body upon pseudopod extension resulting in a cholesterol-free pseudopod (arrows). (iii and vi) Spermatids labeled with NBD-phosphatidylcholine (NBD-PC) showed an even distribution of the fluorophore in spermatids and an NBD-labeled pseudopod (arrows).

these microdomains redistribute resulting in a cholesterol-free pseudopod. Thus, we reasoned that the integrity of membrane microdomains must be important to regulate spermatid activation.

To test whether the amount of cholesterol in spermatids is important for the regulation of sperm activation, we used a perfusion chamber to activate spermatids and induce pseudopod extension. For counting purposes, spermatids were observed by phase contrast microscopy since the pseduopod of activated spermatids appears as a phase-dark protrusion from the bright cell body (see Supplementary Fig. SF3A and Supplementary materials and methods). Spermatids isolated in sperm medium (SM) showed a low proportion of cells that undergo spontaneous pseudopod extension under conditions that promote activation (1.5% ± 0.4 SE for SM; see Fig. 2 A and Supplementary Table ST1). Pseudopod extension was then induced using the known *in vitro* activators Pronase, Monensin and Triethanolamine (TEA) at previously published optimal concentrations [4,34] (see Supplementary materials and methods). Spermatid *in vitro* activation using Pronase induced pseudopod extension in 96% (±1 SE) of spermatids, while Monensin induced pseudopod extension in 85% (±3 SE) of spermatids. TEA was the least effective activator, inducing pseudopod extension in only 52% (±1 SE) of the spermatids. Subsequently, the amount of cholesterol in spermatids was saturated prior to *in vitro* activation. Cholesterol saturation in Pronase-induce activation resulted in the extension of longer "spike" protrusions and an aberrant pseudopod in the majority of cells (88% ± 5 SE; see Fig. 2B, Supplementary Table ST1 and Supplementary video SV4). In the case of Monensin and TEA activation, cholesterol saturation reduced pseudopod extension to 1.3% (±0.5 SE) and 6% (±2 SE), respectively (see Fig. 2B and Supplementary Table ST1). In these experiments, abolishment of pseudopod extension was specific to the effect of cholesterol saturation since preincubation of 2-OH-CD (to sequester the cholesterol present in the media) rescued the inhibition of pseudopod extension (see Supplementary Fig. SF4 and Supplementary Table ST1).

We also tested whether cholesterol depletion from spermatids using the known cholesterol acceptors, β-cyclodextrins or Bovine Serum Albumin (BSA), would increase the proportion of cells undergoing pseudopod extension. Treatment of spermatids with 2OH-CD, methyl-β-cyclodextrin (m-CD), or BSA did not induce spontaneous pseudopod extension (see Supplementary Fig. SF4 and Supplementary Table ST1), suggesting that cholesterol efflux from the spermatid plasma membrane is not sufficient to initiate spermatid activation. A significant increase in the proportion of cells that extended a pseudopod was observed only in spermatids activated with TEA (see Fig. 2B and Supplementary Table ST1). In

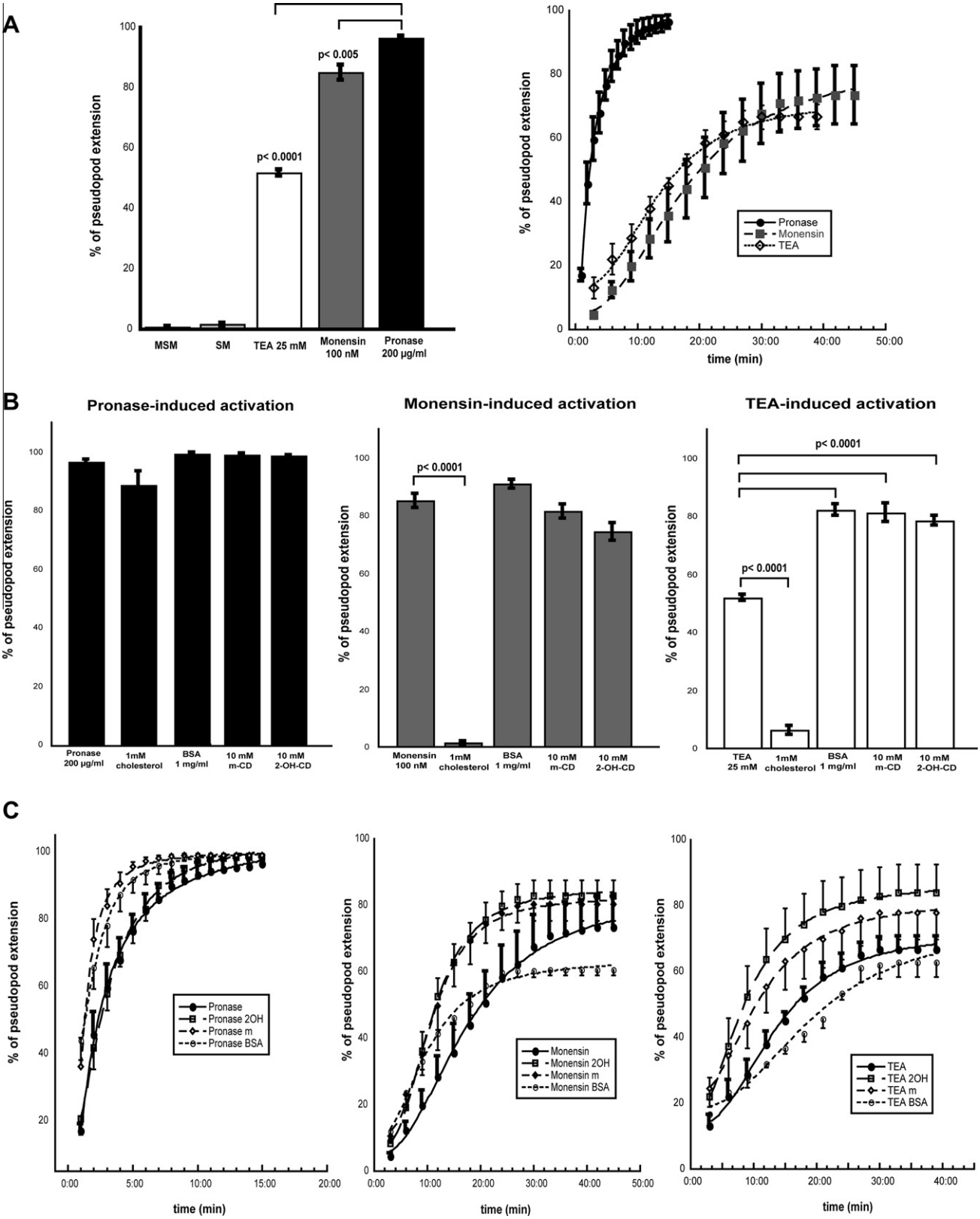

Fig. 2. Effect of cholesterol depletion on *in vitro*-induced pseudopod extension. (A) Proportion of pseudopod extension induced by Triethanolamine (TEA), Monensin or Pronase in spermatids. (B) Proportion of pseudopod extension for each *in vitro* activator after cholesterol saturation or depletion. (C) Kinetics of pseudopod extension for each *in vitro* activator after cholesterol saturation or depletion. Data represents mean ($n = 6$) and error bars depict standard errors (SE). Asterisks represent a statistically significant difference ($p < 0.001$) compared to the control of each *in vitro* activator (for a detailed figure legend see Supplementary information).

this case, the proportion of pseudopod extension increased from 52% (±1 SE) to 82% (±2 SE), 81% (±3 SE) and 78% (±2 SE) for treatments with BSA, m-CD and 2OH-CD, respectively. Together, these results indicate that cholesterol concentration and its discrete

Table 1
Effect of cholesterol depletion on the kinetics of *in vitro* pseudopod extension. Spermatids were treated with cholesterol depletors and *in vitro* pseudopod extension was induced. The time of initial pseudopod extension corresponds to the time at which the first spermatid transitions from cellular rotation and spike extension to pseudopod protrusion. The values of half-time and maximum pseudopod extension were obtained after applying a curve fit to a 4-parameter Hill equation. The coefficient of determination (r^2) and the chi-square values for each curve are given. Control experiment for each *in vitro* activator is in bold followed by their respective treatments. Values are presented in mean ± SE, $n = 6$.

Treatment	Time for initial pseudpod extension after treatment (mean ± SE)	Half-time of pseudopod extension[a] (mean ± SE)	Maximum pseudopod extension[a] (mean ± SE)	Coefficient of determination (r^2)	Chi-square
Pronase (200 μg/ml)	**3.22 ± 0.34** min	**2.44 ± 0.075** min	**102.53 ± 2.15**%	0.99788	0.001557
20H-CD (10 mM)	1.61 ± 0.12 min[d]	2.68 ± 0.09 min	106.55 ± 2.54%	0.99758	0.001945
m-CD (10 mM)	1.00 ± 0.00 min[e]	1.28 ± 0.02 min[f]	99.88 ± 1.15%	0.99703	0.001170
BSA (1 mg/ml)	2.22 ± 0.24 min	1.28 ± 0.04 min[f]	102.89 ± 1.66%	0.99900	0.000350
Monensin (100 nM)	**5.56 ± 0.29** min	**17.50 ± 0.84** min	**84.73 ± 4.22**%	0.99682	0.002595
20H-CD (10 mM)	3.72 ± 0.41 min[c]	10.29 ± 0.24 min[f]	83.65 ± 1.83%	0.99873	0.001124
m-CD (10 mM)	4.50 ± 0.37 min	10.16 ± 0.38 min[f]	80.62 ± 2.82%	0.99733	0.002056
BSA (1 mg/ml)	6.00 ± 0.38 min	8.78 ± 0.53 min[f]	65.32 ± 3.00%	0.92200	0.002651
TEA (25 mM)	**10.5 ± 1.18** min	**13.06 ± 1.59** min	**80.97 ± 7.47**%	0.99578	0.001818
20H-CD (10 mM)	7.44 ± 0.69 min	7.32 ± 0.31 min[c]	91.46 ± 2.60%	0.99964	0.000171
m-CD (10 mM)	5.67 ± 0.61 min[c]	9.19 ± 1.22 min	94.83 ± 6.97%	0.99773	0.000889
BSA (1 mg/ml)	6.94 ± 0.65 min[b]	11.3 ± 1.40 min	67.05 ± 8.93%	0.98078	0.006497

[a] Values obtained after fitting data using a 4-parameter Hill equation.
[b] Statistical difference ($p < 0.05$) of treatment compared to corresponding control.
[c] Statistical difference ($p < 0.015$) of treatment compared to corresponding control.
[d] Statistical difference ($p < 0.01$) of treatment compared to corresponding control.
[e] Statistical difference ($p < 0.005$) of treatment compared to corresponding control.
[f] Statistical difference ($p < 0.001$) of treatment compared to corresponding control.

distribution on the plasma membrane of *C. elegans* spermatids play a role in the regulation of sperm activation and pseudopod extension.

3.3. Cholesterol depletion increases the rate of in vitro-induced pseudopod extension

In order to learn more about the process of pseudopod extension after cholesterol depletion, we used live-cell time-lapse microscopy. Nematode sperm activation can be observed using DIC microscopy since it allows for the observation of cellular details (see Supplementary Fig. SF3B and Supplementary materials and methods). Thus, we followed the kinetics of pseudopod extension after cholesterol depletion and *in vitro* activation. Cholesterol depletion decreased the initial time required for pseudopod extension and increased the rate at which spermatids extended a pseudopod in most treatments and for the three *in vitro* activators (see Table 1 and Supplementary Fig. SF5).

Upon perfusion of Pronase, the spermatids responded rapidly to the stimulus (after 3.2 ± 0.3 min of perfusion) since membrane rearrangements (by cellular rotation), extension of "spikes", pseudopod extension and membrane "ruffling" in the pseudopod were observed (see Supplementary video SV1). The kinetics of Pronase-induced pseudopod extension showed a half-time of 2.44 ± 0.07 min and maximum proportion of pseudopod extension (100%) reached at ~15 min (see Fig. 2C and Table 1). After cholesterol depletion, we observed a ~50% decrease in the initial time for pseudopod extension in the treatments with 2OH-CD and m-CD (see Table 1). A significant difference was also observed in the activation half-time of spermatids treated with m-CD or BSA (1.28 ± 0.03 min and 1.28 ± 0.04 min, respectively; see Fig. 2C, Table 1 and Supplementary Fig. SF5).

In the case of Monensin activation, spermatids responded to the stimulus after 5.6 ± 0.3 min of perfusion. Membrane rearrangements, pseudopod extension and membrane "ruffling" also occurred and spermatozoa were able to crawl (see Supplementary video SV2). Interestingly, after motility acquisition, spermatozoa formed clumps of cells that were disrupted after perfusion of Pronase at the end of the recording. The kinetics of Monensin-induced pseudopod extension revealed a half-time of 17.5 ± 0.8 min and a maximum proportion of pseudopod extension (85 ± 4%) reached at ~45 min (see Fig. 2C and Table 1). Significant differences were observed in the kinetics of cholesterol-depleted spermatids showing a decrease in the initial time of pseudopod extension in 2OH-CD-treated spermatids (3.7 ± 0.4 min) and activation half-times of 10.16 ± 0.4 min for m-CD, 10.3 ± 0.2 min for 2-OH-CD and 8.8 ± 0.5 min for BSA. Maximum pseudopod extension was reached at ~25 min in all treatments (~20 min earlier than the control; see Fig. 2C, Table 1 and Supplementary Fig. SF5).

Spermatid activation induced by TEA effected pseudopod extension slowly after 10.5 ± 1.2 min of perfusion. Membrane rearrangements and "spike" extension were less evident than in Monensin and Pronase-induced activation and some of the cells engaged in cycles of pseudopod extension and retraction prior to pseudopod extension and motility acquisition (see Supplementary video SV3). The kinetics of TEA-induced pseudopod extension showed a curve half-time of 13.1 ± 1.6 min and a maximum proportion of pseudopod extension (81 ± 7.5%) reached at ~30 min (see Fig. 2C and Table 1). In cholesterol-depleted spermatids activated using TEA, cells treated with m-CD and BSA showed a significant reduction in the initial time of pseudopod extension of ~4 min compared to the control (see Table 1) and a significant decrease in the activation half-time of spermatids treated with 2OH-CD (7.3 ± 0.3 min; see Fig. 2C, Table 1 and Supplementary Fig. SF5).

In summary, cholesterol depletion reduced the initial, half- and maximun time of pseudopod extension of *in vitro* activated spermatids. Thus, our results indicate that cholesterol in *C. elegans* spermatids regulate spermatid activation since saturation of cholesterol inhibits this process and cholesterol depletion enhances the rate of pseudopod extension.

4. Discussion

Cholesterol-enriched membrane microdomains play a functional role in the modulation of cytoskeletal dynamics, cell adhesion, and motility, thus, an intimate association among membrane microdomains and the actin-based cytoskeleton has been previously suggested [1,2]. In the MSP-based cytoskeleton of *C. elegans* spermatozoa, proteins from the SPE-8 group form a multicomponent signaling complex that controls the precise timing of pseudopod extension and motility acquisition [35–37]. Early studies using *in vitro* activators have shown that extensive membrane rearrangements and an

intracellular alkalization are necessary and sufficient to induce pseudopod extension in *C. elegans* sperm [3,4,34]. In order to link the genetic and physiological model of pseudopod extension, we propose the involvement of cholesterol-enriched membrane microdomains. In the present study we have identified discrete cholesterol-enriched structures and DRM fractions present in *C. elegans* spermatids, both serving as correlates for the existence of membrane microdomains. These microdomains redistributed towards the cell body and their disruption through cholesterol depletion resulted in an increased rate of pseudopod extension. Further, cholesterol saturation prevented pseudopod extension and the acquisition of motility in spermatids of *C. elegans*. Interestingly, an early study monitored membrane fluidity in *C. elegans* sperm cells using fluorescent recovery after photobleaching (FRAP) [38]. Here the author showed a difference in the diffusion coefficients and fractional fluorescence recoveries between spermatids and spermatozoa ($D \sim 0.7 \times 10^{-10}$ cm^2/sec and ~15% recovery in spermatids compared to $D \sim 2 \times 10^{-10}$ cm^2/sec and ~36% recovery in spermatozoa). This result and our present data are in agreement with a membrane microdomains model in which increasing amounts of cholesterol confer order to the acyl chains of lipids and reduce fluidity of the bilayer [39].

Transcriptionally-inactive flagellated spermatozoa regulate motility and successful fertilization by altering membrane fluidity and permeability through cholesterol depletion [40]. While the crawling spermatozoa from *C. elegans* can appear as a morphological deviation from the "typical" flagellated spermatozoa, this amoeboid cell (using a unique MSP-based cytoskeleton) must regulate motility acquisition and successful fertilization through similar mechanisms as its mammalian counterpart. In this scenario, cholesterol depletion would promote a transition to a fluid state of the plasma membrane in *C. elegans* sperm, inducing an increased rate of spermatid activation, membrane rearrangements, spike protrusion and proper extension of the pseudopod. The opposite effect is then achieved by the addition of cholesterol to the plasma membrane, maintaining a less fluid state and preventing the acquisition of motility in spermatids.

As mentioned previously, exogenous cholesterol is required for reproduction and survival of *C. elegans*. Interestingly, spermatids are part of a subset of cells that preferentially accumulate cholesterol with a putative effect on the structure and physical properties of their plasma membrane [26]. Thus, it would be instructive to direct future experiments towards exploring the effect of cholesterol on physical properties of the membrane such as membrane tension and/or cytoskeletal dynamics of *C. elegans* sperm.

Acknowledgments

We thank Cathrine Castillo, Alejandro Cortez and Haruhiko Miyata for the initial experiments that inspired this work. JJFZ was supported by Grants-in-Aid of Research (GIAR) from Sigma Xi and the Society for Integrative and Comparative Biology. The authors declare no conflict of interest.

Appendix A. Supplementary data

Supplementary data associated with this article can be found, in the online version, at http://dx.doi.org/10.1016/j.bbrc.2012.09.071.

References

[1] T. Golub, S. Wacha, P. Caroni, Spatial and temporal control of signaling through lipid rafts, Current Opinion in Neurobiology 14 (2004) 542–550.
[2] G.R. Chichili, W. Rodgers, Cytoskeleteon-membrane interactions in membrane rafts structure, Cellular and Molecular Life Sciences 66 (2009) 2319–2328.
[3] T.M. Roberts, S. Ward, Membrane flow during nematode spermiogenesis, Journal of Cell Biology 92 (1982) 113–120.
[4] G.A. Nelson, S. Ward, Vesicle fusion, pseudopod extension and amoeboid motility are induced in nematode spermatids by the ionophore monensin, Cell 19 (1980) 457–464.
[5] D.C. Shakes, S. Ward, Initiation of spermiogenesis in *C. elegans*: A pharmacological and genetic analysis, Developmental Biology 134 (1989) 189–200.
[6] T.M. Roberts, M. Stewart, Acting like actin: The dynamics of the nematodemajor sperm protein (MSP) cytoskeleton indicate a push-pull mechanism for amoeboid cell motility, Journal of Cell Biology 149 (2000) 7–12.
[7] T.M. Roberts, S. Ward, Centripetal flow of pseudopodial surface components could propel the amoeboid movement of *Caenorhabditis elegans* spermatozoa, Journal of Cell Biology 92 (1982) 132–138.
[8] B. Geldziler, I. Chatterjee, A. Singson, The gentic and molecular analysis of *spe-19*, a gene required for sperm activation in *Caenorhabditis elegans*, Developmental Biology 283 (2005) 424–436.
[9] A. Minniti, C. Sadler, S. Ward, Genetic and molecular analysis of spe-27, a gene required for spermiogenesis in Caenorhabditis elegans hermaphrodites, Genetics 143 (1996) 213–223.
[10] S.L. L'Hernault, D.C. Shakes, S. Ward, Developmental genetics of chromosome I spermatogenesis-defective mutants in the nematode *Caenorhabditis elegans*, Genetics 129 (1988) 435–452.
[11] J. Nance, A. Minniti, C. Sadler, S. Ward, Spe-12 encodes a sperm cell surface protein that promotes spermiogenesis in Caenorhabditis elegans, Genetics 152 (1999) 209–220.
[12] J. Nance, E.B. Davis, S. Ward, Spe-29 encodes a small predicted membrane protein required for the initiation of sperm activation in Caenorhabditis elegans, Genetics 156 (2000) 1623–1633.
[13] P.J. Muhlrad, S. Ward, Spermiogenesis initiation in *Caenorhabditis elegans* involves a Casein kinase 1 encoded by the *spe-6* gene, Genetics 161 (2002) 143–155.
[14] A. Singson, K.B. Mercer, S.W. L'Hernault, The C. elegans spe-9 gene encodes a sperm transmembrane protein that contains EGF-like repeats and is required for fertilization, Cell 93 (1998) 71–79.
[15] I. Chatterjee, A. Richmond, E. Putiri, D. Shakes, A. Singson, The *Caenorhabditis elegans spe-38* gene encodes a novel four-pass integral membrane protein required for sperm function at fertilization, Development 132 (2005) 2795–2808.
[16] X.-Z.S. Xu, W. Sternberg Paul, A C. elegans sperm TRP protein required for sperm-egg interactions during fertilization, Cell 114 (2003) 285–297.
[17] T.L. Kroft, E.J. Gleason, S.W. L'Hernault, The spe-42 gene is required for sperm-egg interactions during *C. elegans* fertilization and encodes a sperm-specific transmembrane protein, Developmental Biology 286 (2005) 169–181.
[18] A. Singson, JS. Hang, JM. Parry, Genes required for the common miracle of fertilization in *Caenorhabditis elegans*, International, Journal of Developmental Biology 52 (2008) 647–656.
[19] J.J. Fraire-Zamora, R.A. Cardullo, The physiological acquisition of amoeboid motility in nematode sperm: Is the tail the only thing the sperm lost?, Molecular Reproduction and Development 77 (2010) 739–750
[20] F.R. Maxfiled, I. Tabas, Role of cholesterol and lipid organization in disease, Nature 438 (2005) 612–621.
[21] L.M. Pierini, RJ. Eddy, M. Fuortes, S. Seveau, C. Casulo, FR. Maxfield, Membrane lipid organization is critical for human neutrophil organization, Journal of Biological Chemistry 278 (2003) 10831–10841.
[22] C. Gómez-Moutón, JL. Abad, E. Mira, RA. Lacalle, E. Gallardo, S. Jiménez-Baranda, I. Illa, A. Bernad, S. Mañes, -A.C. Martinez, Segregtaion of leading-edge and uropod components into specific lipid rafts during T cell polarization, Proceedings of the National Academy of Sciences of the United States of America 98 (2001) 9642–9647.
[23] S. Mañes, E. Mira, C. Gómoez-Moutón, RA. Lacalle, P. Keller, JP. Labrador, -A.C. Martínez, Membrane raft microdomains mediate front-rear polarity in migrating cells, The EMBO Journal 18 (1999) 6211–6220.
[24] P.E. Visconti, H. Galantino-Homer, X.P. Ning, G.D. Moore, J.P. Valenzuela, C.J. Jorgez, J.G. Alvarez, G.S. Kopf, Cholesterol efflux-mediated signal transduction in mammalian sperm. beta-cyclodextrins initiate transmembrane signaling leading to an increase in protein tyrosine phosphorylation and capacitation., Journal of Biological Chemistry 274 (1999) 3235–3242.
[25] W.F. Hieb, M. Rothstein, Sterol requirement for reproduction of a free-living nematode, Science 170 (1968) 778–780.
[26] T.V. Kurzchalia, S. Ward, Why do worms need cholesterol?, Nature Cell Biology 5 (2003) 684–688
[27] V. Matyash, C. Geier, A. Henske, S. Mukherjee, D. Hirsh, C. Thiele, B. Grant, F.R. Maxfield, T.V. Kurzchalia, Distribution and transport of cholesterol in *Caenorhabditis elegans*, Molecular Biology of the Cell 12 (2001) 1725–1736.
[28] J. Hodgkin, H.R. Horvitz, S. Brenner, Nondisjunction mutants of the nematode *Caeonorhabditis elegans*, Genetics 91 (1979) 67–94.
[29] S. Ward, Y. Argon, G.A. Nelson, Sperm morphogenesis in wild-type and fertilization-defective mutants of Caenorhabditis elegans, Journal of Cell Biology 91 (1981) 26–44.
[30] S. Brenner, The genetics of *Caenorhabditis elegans*, Genetics 77 (1974) 71–94.
[31] J.J. Fraire-Zamora, G. Broitman-Maduro, M. Maduro, R.A. Cardullo, Evidence for phosphorylation in the MSP cytoskeletal filaments of amoeboid spermatozoa, International Journal of Biochemistry and Molecular Biology 2 (2011) 263–273.
[32] D.A. Brown, J.K. Rose, Sorting of GPI-anchored proteins to glycolipid-enriched membrane subdomains during transport to the apical cell surface, Cell 68 (1992) 533–544.

[33] S.L. L'Hernault, T.M. Roberts, Cell biology of nematode sperm, Methods in Cell Biology 48 (1995) 273–301.

[34] S. Ward, E. Hogan, G.A. Nelson, The initiation of spermiogenesis in the nematode *Caenorhabditis elegans*, Developmental Biology 98 (1983) 70–79.

[35] G.M. Stanfield, A.M. Villenueve, Regulation of sperm activation by SWM-1 is required for reproductive success of *C. elegans* males, Current Biology 16 (2006) 252–263.

[36] A. Singson, Sperm activation: time and tide wait for no sperm, Current Biology 16 (2006) R160–R162.

[37] J.R. Smith, G.M. Stanfield, TRY-5 is a sperm-activating protease in *Caeonrhabditis elegans* seminal fluid, PLoS Genetics 7 (2011) e1002375.

[38] Y. Argon, Genetic and biochemical analyses of sperm-defective mutants of *Caenorhabditis elegans*, Dept. of Biological Chemistry Harvard University, Cambridge, MA, 1979. pp. 190.

[39] D.A. Brown, E. London, Structure and origin of ordered lipid domains in biological membranes, Journal of Membrane Biology 164 (1998) 103–114.

[40] G.S. Kopf, PE. Visconti, H. Galantino-Homer, Capacitation of the mammalian spermatozoon, in: P.W. Wassarman (Ed.), Advances in Developmental Biochemistry, JAI Press, Stamford, CT, 1999.